minerals

Article

Age and Tectonic Setting of Layered Lead–Zinc Ore Bodies in the Xiaohongshilazi Deposit: Constraints from Geochronology and Geochemistry of the Volcanic Rocks in Central Jilin Province, NE China

Qun Yang [1], Qingqing Shang [1,*], Yunsheng Ren [2] and Zhongjie Yang [3]

1 College of Earth Sciences, Jilin University, Changchun 130061, China; yangqun@jlu.edu.cn
2 School of Earth Science, Institute of Disaster Prevention, Langfang 065201, China; renys@jlu.edu.cn
3 Mudanjiang Natural Resources Comprehensive Survey Center, China Geological Survey, Mudanjiang 157000, China; yangzj870227@163.com
* Correspondence: shangqq@jlu.edu.cn

Abstract: The newly discovered Xiaohongshilazi deposit located in Panshi City, central Jilin Province, NE China, is a medium-scale Pb–Zn–(Ag) deposit. The Pb–Zn–(Ag) orebodies are divided into layered and vein-type orebodies, which have different ore geneses. The layered Pb–Zn orebodies are mainly hosted within and spatially controlled by the volcanic rocks. To constrain the age and tectonic setting of the layered Pb–Zn mineralization, we completed laser-ablation–ICP–MS zircon U–Pb dating and whole-rock major and trace element analyses of the ore-bearing volcanic rocks. The dacite samples were confirmed as belonging to the Daheshen Formation and were the main ore-bearing volcanic rocks for the layered orebodies. They yielded concordia U–Pb ages of 278.1 $\pm$ 1.8 Ma and 278.3 $\pm$ 1.8 Ma, respectively, indicating that the volcanic rocks from the Daheshen Formation and related layered Pb–Zn mineralization were formed in the early Permian. The andesite and rhyolite located above the layered orebodies yielded concordia U–Pb ages of 225.0 $\pm$ 1.1 Ma, 225.3 $\pm$ 1.5 Ma, and 224.7 $\pm$ 1.2 Ma, respectively; these substances are considered to be of the Sihetun Formation and were first reported in the area. The dacite samples associated with layered Pb–Zn mineralization were high in SiO_2 (62.54–65.02 wt.%), enriched in LREEs and LILEs (e.g., Rb, Ba, and K), and showed depletion in HFSEs (e.g., P and Ti). It showed slightly negative Eu anomalies (δEu = 0.60–0.65) and negative Nb anomalies, with Th/Nb (1.12–1.21) and La/Nb (2.8–4.7) ratios, presenting subduction-related arc magma affinity formed in an active continental margin setting. In agreement with previous studies on zircon Hf isotopes (ε_{Hf} (t) = +0.23~ +10.60) of the volcanic rocks from the Daheshen Formation, we infer that they were derived from the partial melting of the depleted lower crust. In conclusion, mineralization characteristics, geochronological data, geochemical features, and regional tectonic evolution suggest that two Pb–Zn–(Ag) mineralization stages from the Xiaohongshilazi deposit occurred: the layered VMS-type Pb–Zn mineralization associated with the marine volcanic rocks from the early Permian Daheshen Formation, which was induced by the subduction of the Paleo-Asian oceanic plate beneath the northern margin of the North China Craton, and the vein-type Pb–Zn–(Ag) mineralization caused by the subduction of the Paleo-Pacific Plate in the early Jurassic. Considering this, along with the mineralization characteristics of the same-type polymetallic deposits in this region, we propose that the early Permian marine volcanic rocks have great prospecting potential for the VMS-type Pb–Zn polymetallic deposits.

Keywords: LA-ICP-MS zircon U–Pb dating; geochemistry of volcanic rocks; layered Pb–Zn orebodies; Xiaohongshilazi deposit; central Jilin Province

check for updates

Citation: Yang, Q.; Shang, Q.; Ren, Y.; Yang, Z. Age and Tectonic Setting of Layered Lead–Zinc Ore Bodies in the Xiaohongshilazi Deposit: Constraints from Geochronology and Geochemistry of the Volcanic Rocks in Central Jilin Province, NE China. *Minerals* **2023**, *13*, 1371. https://doi.org/10.3390/min13111371

Academic Editor: George M. Gibson

Received: 28 August 2023
Revised: 19 October 2023
Accepted: 25 October 2023
Published: 27 October 2023

1. Introduction

Central Jilin Province, Northeast China, located on the intersection between the eastern segments of the northern margin of North China Craton (NCC) and Xing'an Mongolian

Orogenic Belt (XMOB), experienced the evolution, superposition, and transition of the Paleo-Asian Ocean and Paleo-Pacific Ocean tectonic domains from the late Paleozoic to the early Mesozoic [1–5]. Numerous porphyry Mo deposits, mesothermal hydrothermal lode gold deposits, and magmatic Cu–Ni sulfide deposits have been discovered in this region, and they are temporally and spatially related to the widespread Mesozoic intrusions [6–13]. However, the deposits related to Paleozoic magmatism are relatively scarce and poorly studied in the area. In recent years, Pb–Zn polymetallic deposits (such as the Xiaohongshilazi Pb–Zn deposit, Hongtaiping Pb–Zn–Cu deposit, Dongfengnanshan Pb–Zn–Cu deposit, etc.) occurring in Paleozoic marine volcanic rocks have been discovered along the Solonker–Xra Moron–Changchun–Yanji suture zone [14–17]. The discovery of these deposits can contribute to the study of Paleozoic mineralization in Northeast China and provide a new direction for the exploration of polymetallic deposits in this area, and also has great scientific significance for the study of the evolution and metallogenesis of the Paleo-Asian Ocean.

The newly discovered Xiaohongshilazi deposit is located ~30 km east of Panshi City in central Jilin Province, NE China. It is a medium-scale Pb–Zn–(Ag) deposit containing reserves of 34,968 t Pb, 100,150 t Zn, and 158 t Ag at average grades of 1.39% Zn, 0.486% Pb, and 21.94 g/t Ag [18]. Until recently, studies of the Xiaohongshilazi deposit were still focused on the vein-type orebodies [13,19,20], but the studies on the layered Pb–Zn orebodies were scarce. Based on current research, the vein-type Pb–Zn–(Ag) mineralization is related to an early Mesozoic (~200 Ma) tectono-magmatic–hydrothermal event induced by the initial subduction of the Paleo-Pacific Plate [18–20]. The layered Pb–Zn orebodies have the characteristics of VMS-type mineralization, according to the limited studies of the ore-forming conditions [21,22]. However, significant scientific studies on the layered Pb–Zn orebodies have not been reported so far. Firstly, the layered orebodies are interbedded with the marine volcanic rocks, and clearly cut by the late vein-type orebodies. Nevertheless, the mineralization timing of the layered Pb–Zn ore remains unknown due to the lack of clarity on the age of the ore-bearing volcanic rocks. Secondly, there are two distinct viewpoints about the tectonic setting in this region in the late Paleozoic: (1) the continental rift, taphrogenic trough, and post-orogenic extension after the final closure of the Paleo-Asian Ocean [23–26]; (2) the subduction of the Paleo-Asian oceanic plate beneath the northern margin of NCC [5,8,12,27–32]. It is therefore uncertain whether the layered Pb–Zn mineralization of the Xiaohongshilazi deposit was formed in an extensional setting after the final closure of the Paleo-Asian Ocean or formed in the subduction of the Paleo-Asian oceanic plate. Solving these scientific problems will not only improve understanding of the mineralization process of the Xiaohongshilazi deposit, but will also be important for the study of Paleozoic mineralization in this region and the evolution of the ancient Asian Ocean.

As a result, our focus is on the characteristics of layered Pb–Zn mineralization in the Xiaohongshilazi Pb–Zn–(Ag) deposit. We conducted laser-ablation–ICP–MS zircon U–Pb dating and collected whole-rock major and trace element data from the ore-bearing volcanic rocks to determine the age and tectonic setting of the layered Pb–Zn mineralization. This study holds importance for the research and exploration of similar deposits in this region.

2. Geological Background and Deposit Geology

Located at the junction between the XMOB and the northern margin of NCC, central Jilin Province successively experienced two distinct tectonic evolution stages during the Paleozoic to Cenozoic era [3,5] (Figure 1A). The Paleozoic tectonic evolution was controlled mainly by the progressive subduction of the Paleo-Asian oceanic plate beneath the northern margin of NCC, and the Mesozoic–Cenozoic tectonic evolution was dominated by the oblique subduction of the Paleo-Pacific oceanic plate beneath the Eurasian continent [11,12,30–35]. More than 10 large Mesozoic deposits, including porphyry Mo deposits (Daheishan, Jidetun, and Fu'anbu), lode gold deposits (Toudaochuan and Cuyu), and magmatic Cu–Ni sulfide deposits (Hongqiling), have been discovered in this region.

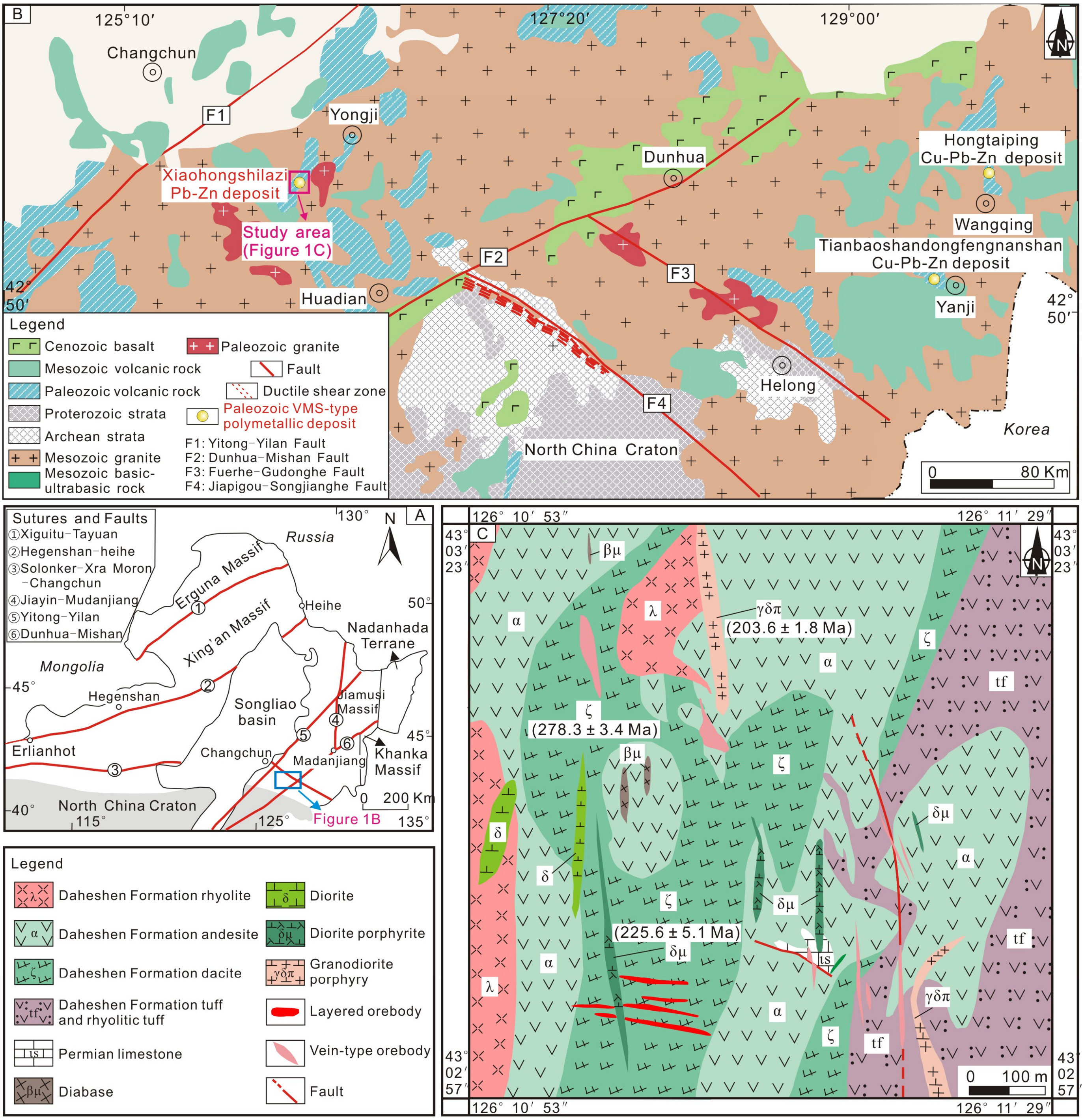

Figure 1. (**A**) Simplified tectonic map of NE China (modified from Wu et al. [2]); (**B**) Regional geological map of the central Jilin Province (modified from Yang [13]). (**C**) Geological map of Xiaohongshilazi Pb–Zn–(Ag) deposit (modified from Yang et al. [20]).

The Xiaohongshilazi deposit in central Jilin Province is located in the southeast segment of the intersection between the Yilan–Yitong fault and the Solonker–Xra Moron–Changchun suture (Figure 1B). The mainly exposed strata in the area are Daheshen Formation volcanic rocks (Figure 1C). The Daheshen Formation is composed of marine intermediate-acidic volcanic rocks, terrigenous clastic rocks, and carbonate rocks, which are locally mixed with a small number of continental clastic rocks. In addition, there are a large number of fusulina fossils, mainly Monodiexodina; plant fossils, mainly Cardioneura;

corals; brachiopods; and bryozoan fossils [13], indicating a marine environment. The volcanic rocks in the Xiaohongshilazi deposit are composed of andesitic volcanic breccia, andesite, dacite, rhyolite, andesitic tuff, dacitic tuff, rhyolitic tuff, etc. (Figure 2A). The micropetrographic characteristics of the volcanic rocks from the Xiaohongshilazi deposit are listed in Table 1 and shown in Figure 3. Dacite interbedded with the layered Pb–Zn orebodies is the primary ore-bearing volcanic rock Figures 2A,B and 4A.

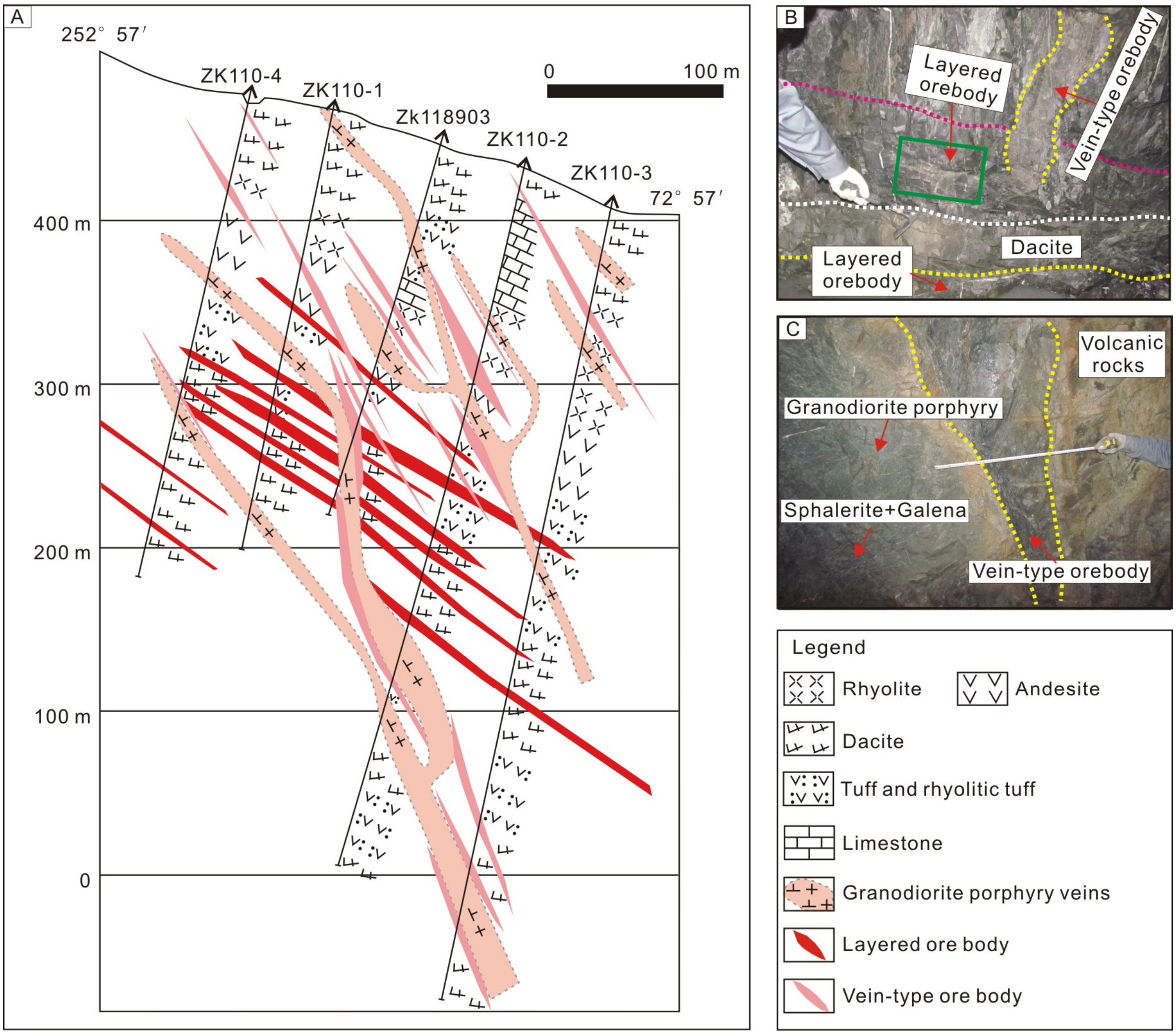

Figure 2. (**A**) Profile map of exploration line from the Xiaohongshilazi Pb–Zn–(Ag) deposit (modified from Chang [18]). (**B**) Vein-type Pb–Zn–(Ag) orebodies cut the layered orebodies and the volcanic rocks; (**C**) vein-type Pb–Zn–(Ag) orebodies occur around the granodiorite porphyry, and both develop along fissures and fractures and cut the volcanic rocks.

Table 1. Characteristics of the volcanic rocks in the Xiaohongshilazi ore district.

Sample No.	Lithology	Location	Texture/Structure	Phenocrysts	Matrix
X370-9	Andesite	370 m-depth of Xifeng mine	Porphyritic texture massive structure	Phenocrysts account for 45% of the rock, and consist of plagioclase (~35%, 2–7.5 mm) and amphibole (~10%, 0.5–4 mm, partly altered to chlorite)	Matrix is primarily pilotaxitic texture and dominated by plagioclase (~0.2 mm) and minor amphibole (~0.2 mm)
7XH-3	Andesite	Above the layered orebodies of Dongfeng mine	Porphyritic texture massive structure	Phenocrysts account for 40% of the rock, and consist of plagioclase (0.25–0.6 mm, partly altered to calcite)	Matrix is primarily pilotaxitic texture and dominated by plagioclase (0.1–0.2 mm) and minor amphibole (~0.1 mm)

Table 1. *Cont.*

Sample No.	Lithology	Location	Texture/Structure	Phenocrysts	Matrix
7XH-4	Rhyolite	Above the layered orebodies of Dongfeng mine	Porphyritic texture rhyolitic structure	Phenocrysts account for 25% of the rock, and consist of quartz (~20%, 0.2–0.5 mm,) and minor sanidine (5%, 0.3–0.4 mm)	Matrix is primarily cryptocrystalline texture and dominated by quartz (~30%), K-feldspar (~25%) and plagioclase
7XH-8-1	Dacite	Interbedding with the layered orebodies of Dongfeng mine	Porphyritic texture massive structure	Phenocrysts account for 55% of the rock, and consist of quartz (15%, ~0.2 mm) and plagioclase (40%, 0.5–2 mm) with minor amphibole	Matrix is primarily microcrystalline texture and dominated by plagioclase and quartz (10%, 0.03–0.1 mm)
7XH-8-2	Dacite	Interbedding with the layered orebodies of Xifeng mine	Porphyritic texture massive structure	Phenocrysts account for 40% of the rock, and consist of quartz (10%, 0.2–0.25 mm), plagioclase (30%, 0.3–2.2 mm) with minor amphibole	Matrix is primarily microcrystalline texture and dominated by plagioclase and quartz (15%, 0.01–0.1 mm)

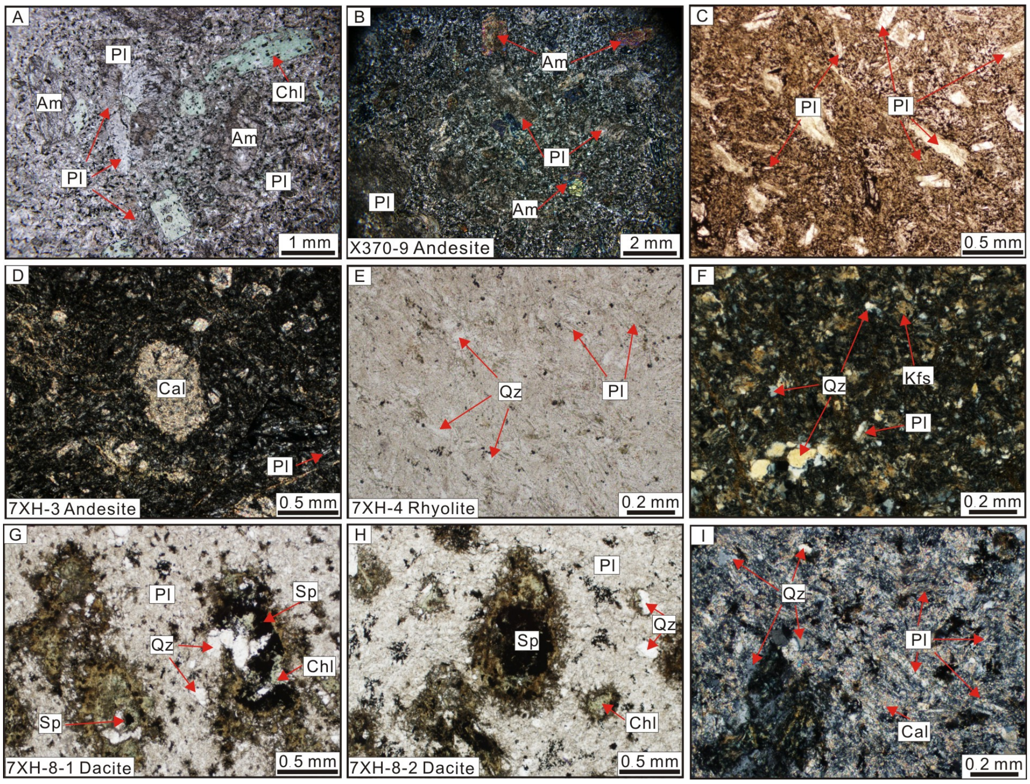

Figure 3. Photomicrographs of the volcanic rocks from Xiaohongshilazi deposit. (**A**,**B**) Andesite (X370-9; A under polarized light; B under cross-polarized light); (**C**,**D**) andesite (7XH-3; C under polarized light; D under cross-polarized light); (**E**,**F**) rhyolite (7XH-4; E under polarized light; F under cross-polarized light); (**G**) dacite (7XH-8-1; polarized light); (**H**,**I**) dacite (7XH-8-2; H under polarized light; I under cross-polarized light). Abbreviations: Sp: sphalerite; Am: amphibole; Pl: plagioclase; Kfs: K-feldspar; Qz: quartz; Chl: chlorite; Cal: calcite.

According to the cross-cutting relationships of the faults, the structures in the ore district can be classified into two groups: (1) the major N–S-trending faults, which controlled the distribution of vein-type Pb–Zn–(Ag) mineralization and intrusions; and (2) the post-mineralization NE–SW-trending faults, which cut the vein-type orebody and intrusions (Figure 1C). The intrusions in the ore district, including diorite porphyry and granodiorite porphyry, with minor diorite and diabase dikes, are commonly N–S-trending and parallel to the vein-type Pb–Zn–(Ag) orebodies (Figure 1C). The granodiorite porphyry (203.6 ± 1.8 Ma, U–Pb zircon) within the internal Pb–Zn mineralization (Figure 4F–G) cut the diorite porphyry (225.6 ± 5.1 Ma, U–Pb zircon), and was closely associated with the vein-type Pb–Zn–(Ag) mineralization of the Xiaohongshilazi deposit (195 ± 17 Ma; sulfide Rb–Sr dating) [20].

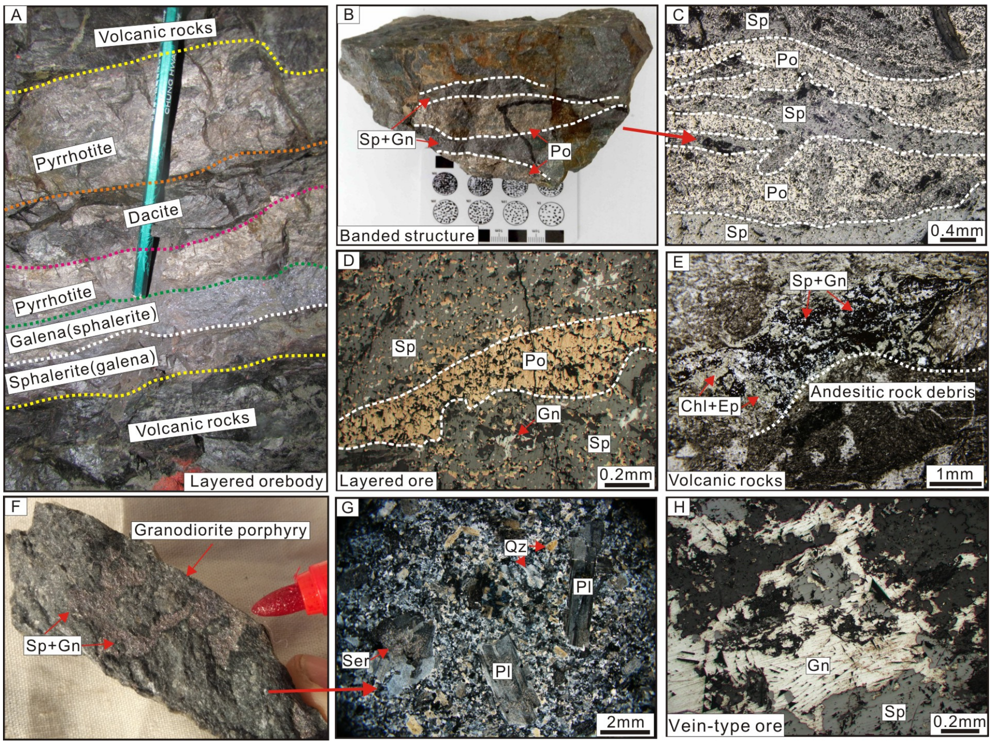

Figure 4. Representative photographs showing the texture and structure of orebodies in the Xiaohongshilazi Pb–Zn–(Ag) deposit. (**A**) Layered Pb–Zn orebodies, displaying a banded structure and interbedding with the volcanic rocks; (**B**) banded structure of the layered ore; (**C**) pyrrhotite interbedded with sphalerite in the layered ore (reflected light); (**D**) pyrrhotite interbedded with sphalerite and minor galena in the layered ore (reflected light); (**E**) chloritization and epidotization associated with layered Pb–Zn mineralization in the volcaniclastic rock (polarized light); (**F**) veinlet Pb–Zn mineralization in the granodiorite porphyry; (**G**) granodiorite porphyry (cross-polarized light); (**H**) sphalerite replaced by galena during the major stage of the vein-type mineralization (reflected light). Abbreviations: Sp: sphalerite; Gn: galena; Po: pyrrhotite; Chl: chlorite; Ep: epidote; Qz: quartz; Pl: plagioclase; Ser: sericite.

Forty-one Pb–Zn–(Ag) orebodies in the ore district were categorized into layered orebodies (n = 19) and vein-type orebodies (n = 22). The layered Pb–Zn orebodies that were mainly hosted within and spatially dominated by volcanic rocks were cut by vein-type Pb–Zn–(Ag) orebodies (Figure 2), which had lengths of 100–400 m, depths of 110–280 m, and thicknesses of 1–3 m in the ore district [18,19,22]. In addition, the ore fabrics, mineral assemblages, and wall-rock alteration showed obvious differences between the layered and vein-type ores. Layered ore occurred mainly as a banded structure (Figure 4A–D), and the vein-type ore displayed a vein structure (Figure 2C). The metallic minerals in layered ore were mainly composed of sphalerite, galena, pyrrhotite (Figure 4A–D), pyrite, and minor chalcopyrite, and those in the vein-type ore dominantly consisted of galena, sphalerite (Figure 4F,H), pyrite, and silver. In contrast with the metallic minerals of layered ore, pyrrhotite and chalcopyrite were not found in the vein-type ore. Moreover, the layered ore had more sphalerite, while the vein-type ore had more galena. Accompanied by Pb–Zn mineralization in the layered ore, most of the crystal and rock fabric in the volcanic rocks, including biotite, amphibole, plagioclase, and andesitic rock fabric, had been altered to chlorite, epidote, and calcite minerals (Figure 4E). The wall-rock alteration related to the layered Pb–Zn mineralization would have been controlled by the reaction between the marine volcanic rocks and hot brine, because the layered orebodies were interbedded with the marine volcanic rocks (Figure 4A). The volcanic rocks and the layered orebodies were cut by the vein-type Pb–Zn–(Ag) mineralization along fractures and fissures that mainly occurred at the edge of the granodiorite porphyry (Figure 2B,C). In the granodiorite porphyry, the primary plagioclase, biotite, and amphibole had been altered to become hydrothermal quartz, chlorite, epidote, sericite, and calcite (Figure 4G), which was related to vein-type Pb–Zn–(Ag) mineralization and most likely dominated by the reaction between ore-bearing hydrothermal fluids and rock-forming minerals of the granodiorite porphyry. The silicification related to vein-type Pb–Zn–(Ag) mineralization, forming abundant quartz-polymetallic sulfide veins, was not found in the layered Pb–Zn mineralization, indicating that the ore geneses of the layered and vein-type orebodies were different.

3. Sample and Analytical Methods

3.1. LA–ICP–MS Zircon U–Pb Dating

More than 100 zircon grains from each volcanic rock in the Xiaohongshilazi ore district (Table 1), were extracted using magnetic and heavy liquid separation techniques, and then handpicked under a binocular microscope at the Integrity Geological Service Corporation in Langfang City, Heibei Province, China. The handpicked zircon grains were mounted in the epoxy resin disk and polished to about half their thickness for exposing crystal cores. Photomicrographs of the zircon grains were taken under reflected and transmitted light. Cathodoluminescence (CL) images of the zircon grains were obtained using a JEOL scanning electron microscope, and used to exhibit their internal structures and determine the spot locations for zircon U–Pb isotope analyses. The spot locations should be selected as far as possible on the growth zoning of zircon grains without inclusions and cracks (Figure 5).

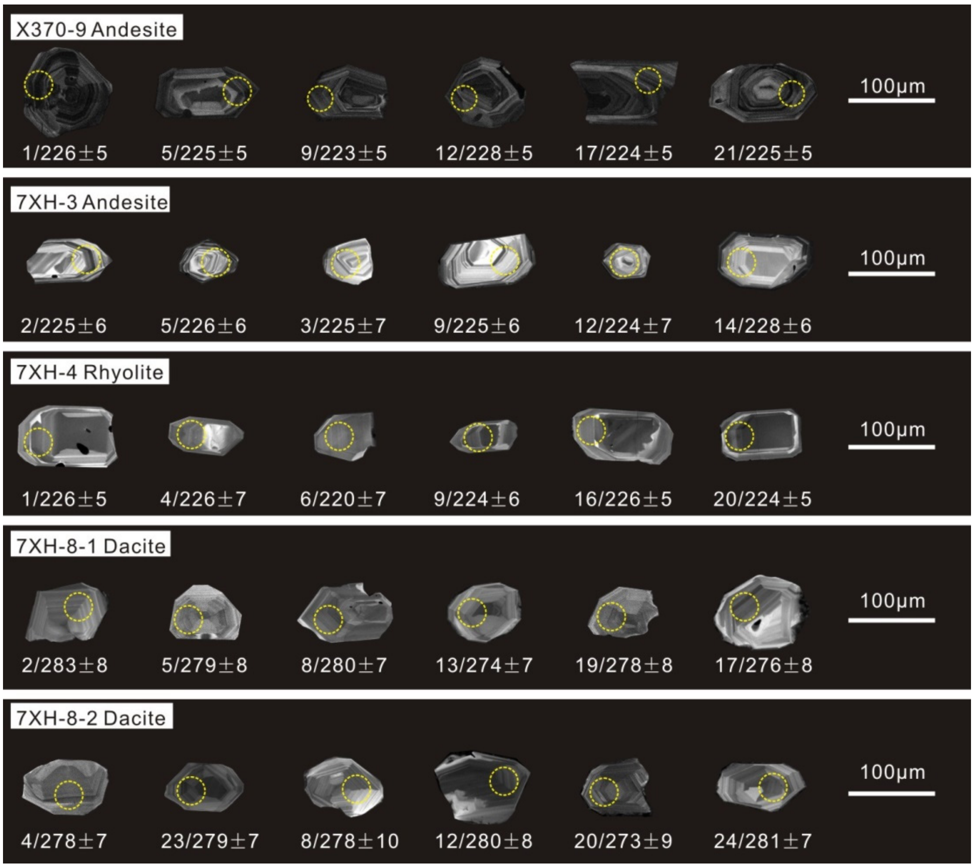

Figure 5. Cathodoluminescence (CL) images of representative zircon grains from the andesite (X370-9 and 7XH-3), rhyolite (7XH-4), and dacite (7XH-8-1 and 7XH-8-2) of the Xiaohongshilazi deposit. Yellow circles denote the locations for U–Pb dating.

Laser ablation (LA)–ICP–MS zircon U–Pb dating for more than 20 zircon grains from each volcanic rock was completed at the Key Laboratory of Mineral Resources Evaluation in Northeast Asia, Ministry of Land and Resources of China, Changchun, Jilin Province, China. The instrument for LA–ICP–MS zircon U–Pb analyses couples a quadrupole ICP–MS (Agilient 75,00c) and 193-nm ArF Excimer laser (COMPexPro 102, Coherent, DE, Saxonburg, Pennsylvania) with the automatic positioning system. The diameter of the laser spot was 32 μm. One zircon standard (91,500) and National Institute of Science and Technology (NIST) 610 reference standard were analyzed after each set of five unknown analyses. The external zircon standard (91,500) was used to correct for isotope ratio fractionation. The NIST610 reference standard was used in the calculations of element concentrations and Si was used as an internal standard. Uncertainties on isotope ratios and ages are presented as $\pm 2\sigma$. The analytical process was described in detail by Hou et al. [36]. The isotope data were calculated using the Glitter 4.0 [37]. Concordia and weighted-mean age diagrams were produced using Isoplot 3.0 [38]. Corrections for common lead were carried out by the method of Andersen [39].

3.2. Major and Trace Element Concentrations

Removing the weathered surfaces, 10 fresh rock samples from the rhyolite (7XH-4) and dacite (7XH-8-1 and 7XH-8-2) were crushed, cleaned repeatedly with deionized water, pulverized, and ground to 200 mesh using an agate mill. Major and trace elements analyses were completed at the State Key Laboratory of Ore Deposit Geochemistry, Institute of Geochemistry, Chinese Academy of Sciences (IGCAS), Guiyang, China. Major and trace element concentrations were determined by the PANalytical Axios-advance X-ray fluorescence spectrometer (XRF) and Perkin-Elmer-ELAN 6000 inductively coupled plasma Mass Spectrometer (ICP–MS), respectively. The analysis error is less than 5%. Detailed experimental operation process and method were described by Qi and Zhou [40].

4. Analytical Results

4.1. Zircon U–Pb Age

LA–ICP–MS zircon U–Pb ages for the andesite (X370-9 and 7XH-3), rhyolite (7XH-4) and dacite (7XH-8-1 and 7XH-8-2) are listed in Supplementary Table S1 and shown in Figure 6. All zircon grains from the five volcanic rock samples were euhedral–subhedral in shape and transparent, and mostly displayed oscillatory growth zoning in CL images (Figure 5) and high Th/U ratios (0.34–0.87; Supplementary Table S1), indicating their magmatic origin [41–43].

For sample X370-9, except for one analytical spot showing a $^{206}Pb/^{238}U$ age of 279 ± 6 Ma, 20 analytical spots yielded $^{206}Pb/^{238}U$ ages ranging from 223 ± 5 Ma to 228 ± 5 Ma, with a concordia U–Pb age of 225.0 ± 1.1 Ma (Figure 6A) and a weighted mean age of 225.0 ± 2.2 Ma (MSWD = 0.055, n = 20; Figure 6B). The $^{206}Pb/^{238}U$ ages of 18 analytical spots from sample 7XH-3 varied from 222 ± 9 Ma to 228 ± 6 Ma, with a concordia U–Pb age and a weighted mean age of 225.3 ± 1.5 Ma (Figure 6C) and 225.5 ± 2.9 Ma (MSWD = 0.032, n =18; Figure 6D), respectively. Twenty-five analytical spots from sample 7XH-4 yielded $^{206}Pb/^{238}U$ ages ranging from 220± 7 Ma to 226 ± 7 Ma, and a concordia U–Pb age of 224.7 ± 1.2 Ma (Figure 6E) and a weighted mean age of 224.7 ± 2.3 Ma (MSWD = 0.063, n =25; Figure 6F). From sample 7XH-8-1, the $^{206}Pb/^{238}U$ ages of 20 analytical spots ranged from 274 ± 7 Ma to 284 ± 7 Ma, yielding a concordia U–Pb age of 278.1 ± 1.8 Ma (Figure 6G) and a weighted mean age of 278.3 ± 3.4 Ma (MSWD = 0.16, n = 20; Figure 6H). Twenty-four analytical spots from sample 7XH-8-2 yielded $^{206}Pb/^{238}U$ ages varying from 273 ± 9 Ma to 282 ± 13 Ma, which gave a concordia U–Pb age of 278.3 ± 1.8 Ma (Figure 6I) and a weighted mean age of 278.3 ± 3.4 Ma (MSWD = 0.063, n = 24; Figure 6J). The older zircon grain (279 ± 6 Ma) from sample X370-9 was interpreted to be the crystallization age of inherited or captured zircon entrained by the magma.

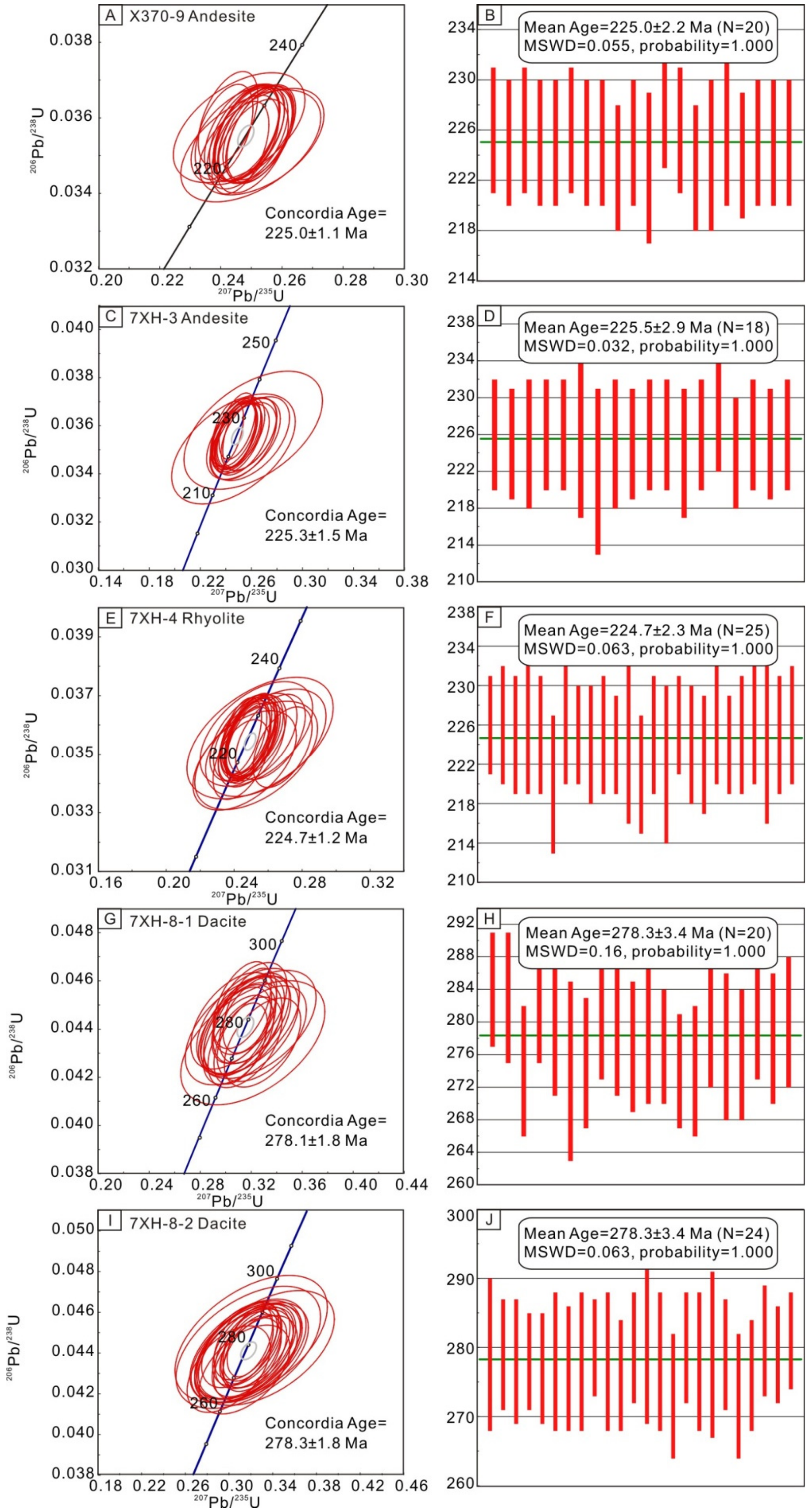

Figure 6. LA–ICP–MS zircon U–Pb diagrams of the concordia age and weighted mean age for the andesite ((**A**,**B**) X370-9; (**C**,**D**) 7XH-3), rhyolite ((**E**,**F**) 7XH-4), and dacite ((**G**,**H**) 7XH-8-1; (**I**,**J**) 7XH-8-2) from the Xiaohongshilazi deposit.

4.2. Major and Trace Element

The whole-rock major and trace element concentrations of the rhyolite (7XH-4) and dacite (7XH-8-1 and 7XH-8-2) from the Xiaohongshilazi deposit are listed in Supplementary Table S2. The rhyolite had high SiO_2 (73.70–76.44 wt.%) and $Na_2O + K_2O$ (7.31–7.64 wt.%), and contained a Al_2O_3 content of 12.76–13.09 wt.%, a TFe_2O_3 content of 1.54–2.89 wt.%, a CaO content of 0.22–0.47 wt.%, a TiO_2 content of 0.12–0.20 wt.%, and a MgO content of 0.68–0.87 wt.%, with Mg# [Mg# = 100 × $Mg^{2+}/(Mg^{2+} + TFe^{2+})$] values varying from 31.62 to 50.51. Compared with the rhyolite, the dacite possessed relatively low SiO_2 ratios ranging from 62.54 to 65.02 wt.% and $Na_2O + K_2O$ varying from 5.23 to 5.45 wt.%, but relatively high Al_2O_3 (15.45–15.71 wt.%), TFe_2O_3(7.97–9.16 wt.%), CaO (0.82–1.25 wt.%), and TiO_2 (0.56–0.68 wt.%), and similar MgO (0.76–0.81 wt.%), with lower Mg# values ranging from 14.88 to 16.12. Their A/CNK ratios varied from 1.30 to 1.36 and ranged from 1.66 to 1.82, respectively, which is indicative of peraluminous rocks.

In the chondrite-normalized rare earth element (REE) patterns (Figure 7A), the rhyolite and dacite samples from the Xiaohongshilazi deposit had different degrees of enrichment in light rare-earth elements (LREEs), relative to heavy rare-earth elements (HREEs). The dacite samples [LREE/HREE = 9.63–13.80, $(La/Yb)_N$ = 9.02–15.55] were more fractionated than the rhyolite samples [LREE/HREE =5.37–6.71, $(La/Yb)_N$ = 3.94–5.15]. The rhyolite had obviously negative Eu anomalies (δEu = 0.04–0.13), while the dacite showed slightly negative Eu anomalies (δEu = 0.60–0.65). In the primitive mantle-normalized geochemical patterns (Figure 7B), both of them were enriched in large-ion lithophile elements (LILEs, e.g., Rb, Ba, and K) with obviously negative Nb, Sr, P, and Ti anomalies. The rhyolite, relative to the dacite, displayed more intense depletion in high-field-strength elements (HFSEs, e.g., P and Ti) and more enrichment in Zr and Hf. The rhyolite and dacite samples were divided into the subalkaline series, and mainly plotted into the rhyolite and dacite regions, respectively, on the Nb/Y vs. Zr/TiO_2*0.0001 diagram (Figure 8A). They were classified as high-K calc-alkaline and shoshonite series, respectively, on Co vs. Th and SiO_2 vs. K_2O diagrams (Figure 8B,C).

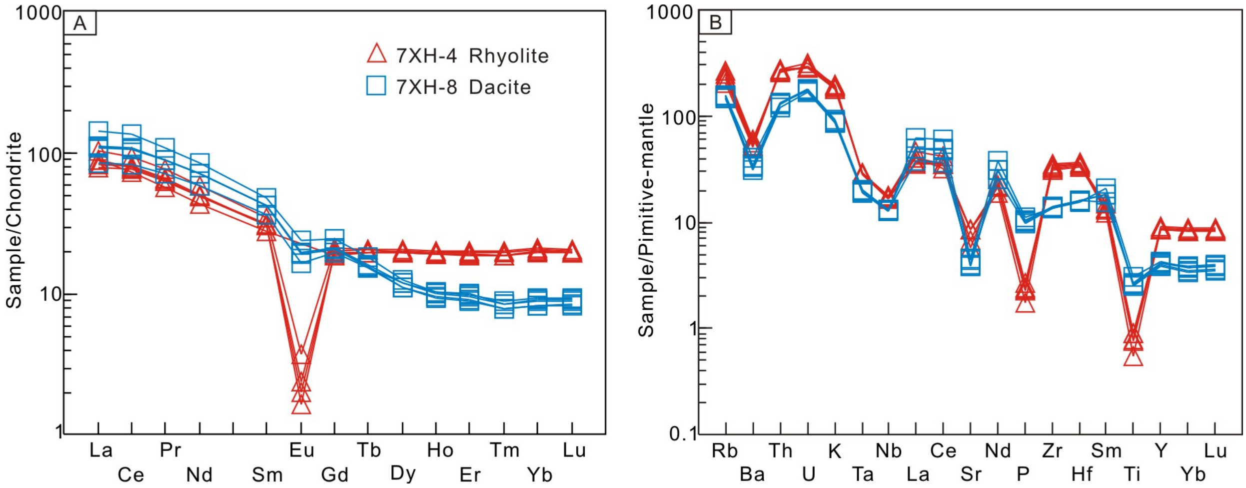

Figure 7. (**A**) Chondrite-normalized rare earth element (REE) patterns and (**B**) primitive mantle-normalized geochemical patterns for the rhyolite and dacite from the Xiaohongsilazi deposit. Chondrite and primitive-mantle values are from Boynton [44] and Sun and McDinough [45], respectively.

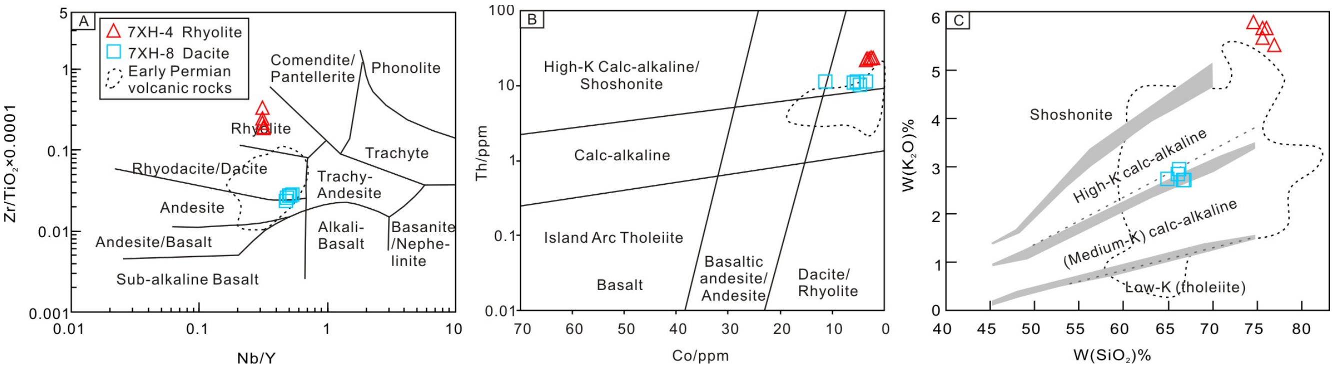

Figure 8. (**A**) Nb/Y vs. $Zr/TiO_2 \times 0.0001$ diagram (modified from Winchester and Floyd [46]); (**B**) Co vs. Th diagram (modified from Hastie et al. [47]); (**C**) SiO_2 vs. K_2O diagram (modified from Peccerillo and Taylor [48]). The data of early Permian volcanic rocks in the area are from Hou [16], Cao [49], and Yu et al. [50].

5. Discussion

5.1. Age of Magmatic Hydrothermal Events and Layered Pb–Zn Mineralization

The dacite samples from Dongfeng and Xifeng mine of Xiaohongshilazi ore district yielded concordia U–Pb ages of 278.1 ± 1.8 Ma and 278.3 ± 1.8 Ma, respectively, indicating that the dacite formed during the early Permian. The andesite and rhyolite samples yielded concordia U–Pb ages of 225.0 ± 1.1 Ma, 225.3 ± 1.5 Ma and 224.7 ± 1.2 Ma, respectively, and were identical within error to the age of diorite porphyry from the Xiaohongshilazi deposit (225.3 ± 5.1 Ma) (Yang et al., 2020). This would suggest that the intermediate-silicic magmatic hydrothermal event in the area occurred during late Triassic time. In addition, one zircon grain from the andesite furnished a $^{206}Pb/^{238}U$ age of 279 ± 6 Ma comparable to that of the dacite samples, indicating that the magmatic zircon from the early Permian was inherited or captured. The ages of the dacite samples (~278.3 Ma) were obviously older than the andesite and rhyolite samples (~225 Ma). These data combined with the distribution of strata in different epoch and their rock types in central Jilin Province [13,51] meant that the dacite samples (~278.3 Ma) could be classified as Daheshen Formation, and the andesite and rhyolite samples (~225 Ma) could be confirmed as Sihetun Formation. The volcanic rocks from the Sihetun Formation were first reported in this area, which provided new geological information for regional geological mapping of central Jilin Province.

As mentioned above, the layered Pb–Zn orebodies were mainly hosted within and controlled by Daheshen Formation and Sihetun Formation volcanic rocks. Nevertheless, the volcanic rocks from the Daheshen Formation were spatially, temporally, and genetically related to the layered Pb–Zn mineralization, which is evidenced by the following: (1) Dacite samples of the Daheshen Formation from Dongfeng and Xifeng mine in the Xiaohongshilazi ore district were all interbedded with the layered orebodies (Figures 2B and 4A). (2) The volcanic rocks from the Daheshen Formation and the layered orebodies were overlain by the volcanic rocks from the Sihetun Formation (~225Ma), and both of them were cut by the vein-type Pb–Zn–(Ag) orebodies and the granodiorite porphyry (~200Ma) (Figure 2A) [20]. (3) No Pb–Zn mineralization was found in the rhyolite and andesite from the Sihetun Formation (Figure 3A–F). (4) In addition to the Xiaohongshalazi deposit, several newly discovered VMS-type polymetallic deposits in this region all occurred in the marine volcanic rocks from the early Permian, such as the Hongtaiping Pb–Zn–Cu deposit, the Dongfengnanshan Pb–Zn–Cu deposit, etc. The zircon U-Pb ages of dacite samples from the Daheshen Formation in the Xiaohongshilazi deposit was consistent with the sphalerite Rb–Sr isochron age of the layered ore from Hongtaiping deposit [52]. In summary, the volcanic rocks from the Daheshen Formation have a closely genetic relationship with the layered Pb–Zn mineralization, suggesting that the layered Pb–Zn mineralization of the Xiaohongshilazi deposit occurred during the early Permian (~278 Ma).

In light of the research of the vein-type Pb–Zn–(Ag) mineralization in the Xiaohongshilazi deposit (~200 Ma) [20], it can be concluded that there were three stages of tectono-magmatic–hydrothermal events that occurred in the Xiaohongshilazi area from the early Permian to the early Jurassic: (1) the early Permian (~278 Ma) forming of the Daheshen Formation marine volcanic rocks related to the layered Pb–Zn mineralization; (2) the late Triassic (~225 Ma) forming of the Sihetun Formation volcanic rocks and the diorite porphyry dikes; (3) the early Jurassic (~200 Ma) forming of the granodiorite porphyry associated with the vein-type Pb–Zn–(Ag) mineralization.

5.2. Tectonic Setting and Associated Mineralization

The dacite from the Daheshen Formation genetically related to the layered Pb–Zn mineralization was geochemically distinguished by high SiO_2, high K, and high Al_2O_3 composition, and was identified as a peraluminous high-K calc-alkaline rock (σ < 3.3 wt.%, Figure 8B,C). The dacite was characterized by an enrichment in LREEs and LILEs (e.g., Rb, Ba, and K), and a depletion in HFSEs (e.g., P and Ti), suggesting that this dacite was formed in a subduction-related tectonic environment as island arc rocks. The Th/Nb (1.12–1.21) and La/Nb (2.8–4.7) ratios (Supplementary Table S2) presented arc magmas that could have been contributed by crustal source contents [53–55]. Meanwhile, the dacite had obviously negative Nb anomalies and slightly negative Eu anomalies (δEu = 0.60–0.65), differing markedly from mantle-derived rocks with strong negative Eu anomalies, indicating that the magma was derived from the crust [56]. The Mg# values (14.88–16.12) of the dacite were lower than those of mantle-derived rocks (Mg# > 40), further implying that it was formed by the partial melting of basaltic lower crust [57]. Moreover, the zircon $\varepsilon_{Hf}(t)$ values of the volcanic rocks from the Daheshen Formation were all positive ($\varepsilon_{Hf}(t)$ = + 0.23~ + 10.60), and Hf two-stage model ages (T_{DM2}) ranged from 1384 Ma to 662 Ma [49,50], suggesting that the original magma was derived from the partial melting of the depleted basaltic lower crust newly accreted during the Meso-Neoproterozoic, which is generally consistent with the Proterozoic accretionary event in this region [58]. In summary, we conclude that the volcanic rocks from the Daheshen Formation most likely originated from the partial melting of depleted lower crust.

The rhyolite from the Sihetun Formation was classified as a peraluminous shoshonitic volcanic rock (Figure 8B,C) with high SiO_2 and high-K (Na_2O/K_2O = 0.28–0.34), and was characterized by an intense enrichment in LREEs and LILEs and a depletion in HFSEs, as well as obviously negative Eu anomalies (δEu = 0.04–0.13) and negative Nb, Sr, P, and Ti anomalies. These geochemical features were similar to A-type rhyolites, and implied that the rhyolitic magma was likely derived from the partial melting of the lower crust, accompanied by the crystallization differentiation of minerals, such as plagioclase, apatite, sphene, etc. [59–61].

The dacite samples are plotted within the field of the volcanic arc granites on the Yb vs. Ta and Y + Nb vs. Rb diagrams (Figure 9A,B), mainly near the region of the active continental margin (continental arc) on the Ta/Yb vs. Th/Yb diagram (Figure 9C). The dacite samples displayed LILE-enrichment and HFSE-depletion, as well as obvious Ta–Nb–Sr–P–Ti troughs, which provide a scenario for a subduction setting similar to the active continental margin. Meanwhile, the tectonic setting of Hongtaiping and Dongfengnanshan VMS-type Pb–Zn–Cu deposits, which had the same ore genesis as the layered Pb–Zn mineralization of the Xiaohongshilazi deposit, indicated an active continental margin [15,50]. Furthermore, a large amount of geochronology data, geochemistry characteristics, and regional tectonic evolution indicated that this region was under an active continental margin arc setting in the early Permian, which related to the southward subduction of the Paleo-Asian oceanic plate beneath the North China Craton [16,17,27–32,49,50,62]. We propose, therefore, the dacite and associated layered Pb–Zn mineralization formed in the subduction setting of the Paleo-Asian oceanic plate in the early Permian (~278 Ma; Figure 10A). The rhyolite samples were plotted close to the field of the within-plate granites and post-orogenic setting in the discrimination diagrams of Yb vs. Ta diagram (Figure 9A), Y + Nb vs. Rb diagram (Figure 9B) and R1 vs. R2 diagram (Figure 9D), respectively. Moreover, the rhyolite displayed an affinity to A-type rhyolites in its geochemical composition, proving that it was formed in the post-collisional extensional setting after the final closure of the Paleo-Asian Ocean. In addition, the existence of bimodal volcanic rocks and A-type rhyolites in the eastern Heilongjiang–Jilin provinces during the late Triassic [5], as well as Hongqiling magmatic Cu–Ni sulfide deposit in the XMOB (~223 Ma) [8,63], further indicate that this region evolved into a period of post-collisional extensional setting involving lithosphere delamination in the late Triassic (Figure 10C). The granodiorite porphyry associated with the vein-type Pb–Zn–(Ag) mineralization was emplaced in the initial subduction stage of the Paleo-Pacific plate in the early Jurassic (~200 Ma; Figure 10D) [20].

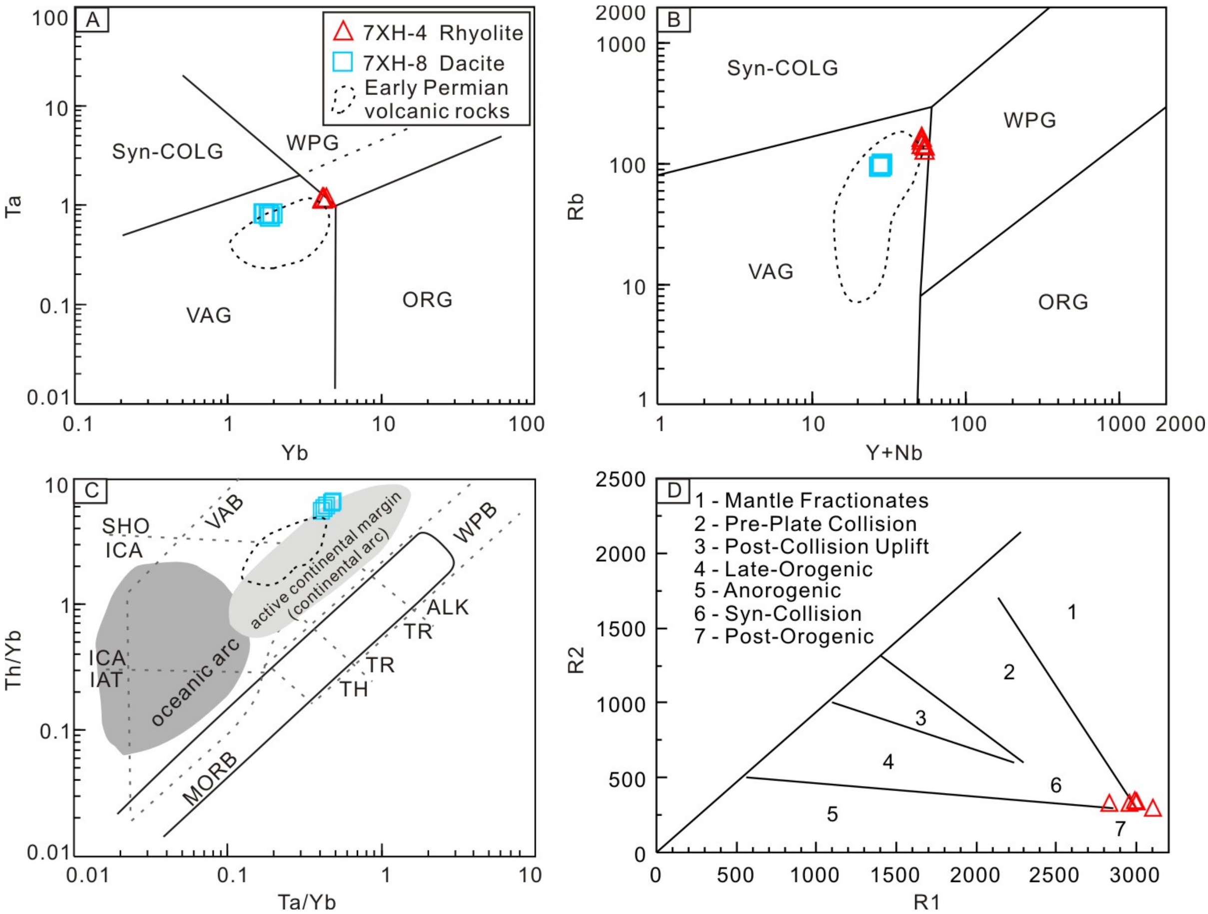

Figure 9. (**A**) Yb vs. Ta diagram (modified from Pearce et al. [64]); (**B**) Y + Nb vs. Rb diagram (modified from Pearce et al. [64]); (**C**) Ta/Yb vs. Th/Yb diagram (modified from Pearce et al. [65]); (**D**) R1 vs. R2 (modified from Batchelor and Bowden [66]); R1 = 4Si−11(Na + K)−2(Fe + Ti) and R2 = 6Ca + 2 Mg + Al). The data of early Permian volcanic rocks in the area are from Hou [16], Cao [49], and Yu et al. [50]. Abbreviations: VAG: volcanic arc granites; Syn-COLG: syn-collisional granites; WPG: within-plate granites; ORG: ocean ridge granites; SHO: shoshonitic series; ICA: island calc-alkaline series; IAT: island arc tholeiites; VAB: volcanic arc basalts; WPB: within-plate basalts; MORB: mid-ocean ridge basalts; ALK: alkalic series; TR: transitional series; TH: tholeiitic series.

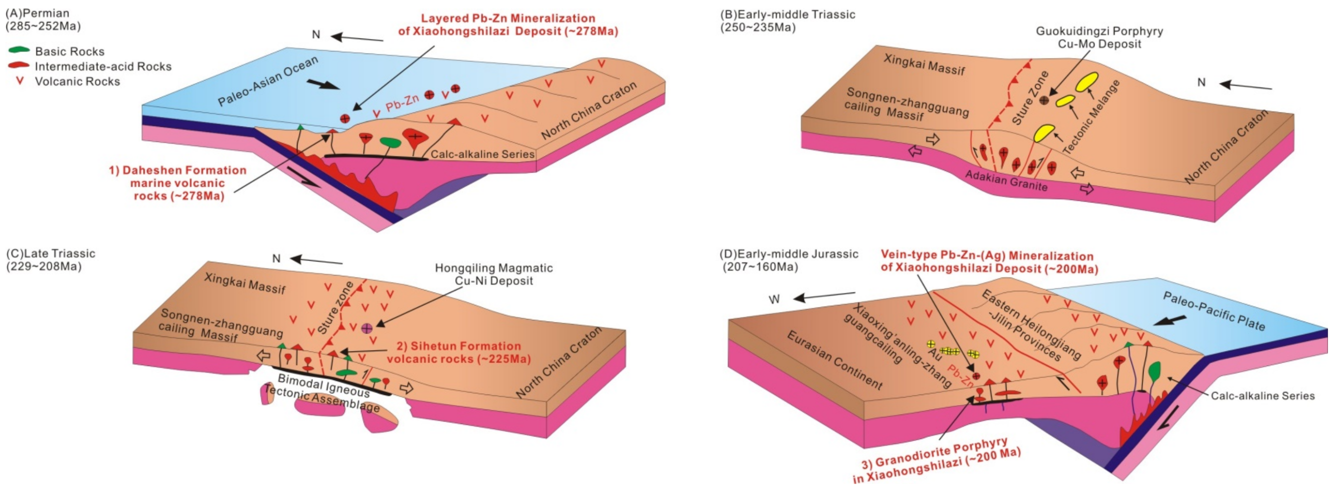

Figure 10. Cartoon block diagrams showing the tectonic evolution and associated mineralization in this region (modified from Yang [13]).

5.3. Implication for the Late Paleozoic Pb–Zn Polymetallic Mineralization

Located on the intersection between the Central Asian Orogenic Belt and the eastern segments of NCC, the central Jilin Province successively experienced the evolution and transition of the Paleo-Asian Ocean and the Paleo-Pacific Ocean metallogenic domains [1–5,30–35]. In the Permian, the sustained subduction of the Paleo-Asian oceanic plate beneath the North China Craton formed the marine volcanic rocks and associated VMS-type polymetallic mineralization (Figure 10A). This area experienced the transition from the collision and closure of the Paleo-Asian Ocean to post-collision extension during the Triassic (Figure 10B,C). Large numbers of Mesozoic polymetallic deposits have been found, including porphyry Cu–Mo deposits (e.g., Guokuidingzi) and magmatic Cu–Ni sulfide deposits (e.g., Hongqiling) [8,58,63]. In the early–middle Jurassic, the regional tectonic setting transformed into the subduction of the Paleo-Pacific oceanic plate beneath the Eurasian continent (Figure 10D), forming mesothermal hydrothermal lode gold deposits (e.g., Cuyu), skarn-type gold deposits (e.g., Guanma), and hydrothermal vein-type Pb–Zn–(Ag) deposits (e.g., Xiaohongshilazi). Nevertheless, few Paleozoic deposits have been discovered. The newly discovered late Paleozoic Pb–Zn polymetallic deposits in Northeast China, including the layered polymetallic mineralization of the Xiaohongshilazi, Hongtaiping, and Dongfengnanshan, are along the Solonker–Xra Moron–Changchun–Yanji suture zone (Figure 1B) and were formed in the active continental margin setting induced by the subduction of the Paleo-Asian Ocean (Figure 10A). The discovery of these deposits is not only helpful to the study of Paleozoic mineralization in this area, but also provides theoretical support for the exploration of the same-type polymetallic deposits and the study of the evolution and associated metallogenesis of the Paleo-Asian Ocean in Northeast China.

At present, the discovered VMS-type mineralization generally occurred in the marine volcanic rocks during the Permian, and no Mesozoic VMS-type deposits have been found in the eastern Heilongjiang–Jilin Provinces, which may be related to the local extension or rifting tectonics under the subduction of the Paleo-Asian oceanic plate in this region during the Paleozoic. Early Permian marine volcanic rocks are the main ore-bearing strata of VMS-type layered mineralization in this area, and they have extremely high zinc background anomaly values [13]. Therefore, the early Permian marine volcanic rocks have large prospecting potential and could be important prospecting indicators for VMS-type polymetallic deposits in this region. In particular, several lead–zinc polymetallic deposits have been found in the marine volcanic rocks of the early Permian Miaoling Formation and Daheshen Formation (Figure 1B). These include the layered Pb–Zn–Cu mineralization of the Hongtaiping and Dongfengnanshan VMS-type deposits in the Yanbian area, eastern

Jilin Province, and the layered Pb–Zn mineralization of the Xiaohongshilazi deposit in Panshi City, central Jilin Province [15,52]. All of these occurred in the early Permian marine volcanic rocks, as seen in Figure 1B. These early Permian marine volcanic rocks related to the Paleo-Asian Ocean evolution are mainly distributed in central (Panshi, Yongji) and eastern (Wangqing, Longjing, Kaishantun) Jilin Province. They represent important lead–zinc polymetallic mineralization areas and are prospecting indicators for VMS-type deposits.

6. Conclusions

(1) The layered Pb–Zn mineralization was interbedded with the volcanic rocks from the Daheshen Formation. It manifested mainly as a banded structure and had more sphalerite than the vein-type mineralization. The dacite samples from the Daheshen Formation yielded concordia ages of 278.1 $\pm$ 1.8 Ma and 278.3 $\pm$ 1.8 Ma, respectively, and were spatially, temporally, and genetically related to the layered Pb–Zn mineralization, indicating that they were formed during the early Permian.

(2) The andesite and rhyolite from the Sihetun Formation yielded ages of 225.0 $\pm$ 1.1 Ma, 225.3 $\pm$ 1.5 Ma, and 224.7 $\pm$ 1.2 Ma, respectively, and were unrelated to the layered Pb–Zn mineralization and first reported in this region.

(3) The Daheshen Formation and Sihetun Formation volcanic rocks were formed in the active continental margin arc setting induced by the subduction of the Paleo-Asian oceanic plate during the early Permian and the post-collisional extensional setting after the final closure of the Paleo-Asian Ocean during the late Triassic, respectively.

(4) Three tectono-magmatic events occurred in the Xiaohongshilazi area during the early Permian (278 Ma), the late Triassic (225 Ma), and the early Jurassic (200 Ma). The layered Pb–Zn mineralization was formed during the early Permian (278 Ma), and the vein-type Pb–Zn–(Ag) mineralization was formed during the early Jurassic (200 Ma).

(5) Early Permian marine volcanic rocks, closely related to the layered Pb–Zn mineralization of VMS-type polymetallic deposits, are important prospecting indicators for similar polymetallic deposits in this region.

Supplementary Materials: The following supporting information can be downloaded at: https://www.mdpi.com/article/10.3390/min13111371/s1, Table S1: LA–ICP–MS zircon U–Pb dating data of the volcanic rocks in the Xiaohongshilazi deposit; Table S2: Whole-rock major and trace element data of the rhyolite and dacite in the Xiaohongsilazi deposit.

Author Contributions: Conceptualization: Q.Y., Q.S. and Z.Y.; field investigation: Q.Y. and Y.R.; experimental analysis: Q.Y. and Z.Y.; software: Q.S.; validation: Q.Y. and Q.S.; resources: Y.R. and Q.Y.; data curation: Q.Y.; writing—original draft preparation: Q.S.; writing—review and editing: Q.Y.; visualization: Q.S.; funding acquisition: Q.Y. and Y.R. All authors have read and agreed to the published version of the manuscript.

Funding: This work was financially supported by the Natural Science Foundation of Jilin Province (no. 20230101089JC) and China Postdoctoral Science Foundation (no. 2022M721305), and the Dynamic Evaluation Project of Gold Resource Potential in Eastern Jilin-Heilongjiang Area (DD20230373).

Data Availability Statement: Not applicable.

Acknowledgments: We would like to thank the leaders and geologists of the Xiaohongshilazi ore district for their support of our fieldwork.

Conflicts of Interest: The authors declare no conflict of interest.

References

1. Wu, F.Y.; Sun, D.Y.; Li, H.M.; Jahn, B.M.; Wilde, S. A-type granites in northeastern China: Age and geochemical constraints on their petrogenesis. *Chem. Geol.* **2002**, *187*, 143–173. [CrossRef]
2. Wu, F.Y.; Sun, D.Y.; Ge, W.C.; Zhang, Y.B.; Grant, M.L.; Wilde, S.A.; Jahn, B.M. Geochronology of the Phanerozoic granitoids in northeastern China. *J. Asian Earth Sci.* **2011**, *41*, 1–30. [CrossRef]
3. Zeng, Q.; Liu, J.; Chu, S.; Wang, Y.; Sun, Y.; Duan, X.; Zhou, L. Mesozoic molybdenum deposits in the East Xingmeng orogenic belt, northeast China: Characteristics and tectonic setting. *Int. Geol. Rev.* **2012**, *54*, 1843–1869. [CrossRef]

4. Zeng, Q.; Liu, J.; Qin, K.; Fan, H.; Chu, S.; Wang, Y.; Zhou, L. Types, characteristics, and time-space distribution of molybdenum deposits in China. *Int. Geol. Rev.* **2013**, *55*, 1311–1358. [CrossRef]
5. Xu, W.L.; Pei, F.P.; Wang, F.; Meng, E.; Ji, W.Q.; Yang, D.B.; Wang, W. Spatial-temporal relationships of Mesozoic volcanic rocks in NE China: Constraints on tectonic overprinting and transformations between multiple tectonic systems. *J. Asian Earth Sci.* **2013**, *74*, 167–193. [CrossRef]
6. Wang, H.; Ren, Y.S.; Zhao, H.L.; Ju, N.; Qu, W.J. Re–Os dating of molybdenite from the Liushengdian Molybdenum deposit in Antu Area of Jilin Province and its geological significance. *Acta Geosci. Sin.* **2011**, *32*, 707–715. (In Chinese with English Abstract)
7. Zhang, Y.; Sun, J.G.; Chen, Y.J.; Zhao, K.Q. Re–Os and U–Pb geochronology of porphyry Mo deposits in central Jilin Province: Mo ore-forming stages in northeast China. *Int. Geol. Rev.* **2013**, *14*, 1763–1785. [CrossRef]
8. Han, C.M.; Xiao, W.J.; Zhao, G.C.; Sun, B.X.; Ao, S.J.; Zhang, J.E.; Wan, B.; Wang, Z.M.; Ding, J.X.; Qu, W.J.; et al. Re–Os isotopic age of the Hongqiling Cu–Ni sulfide deposit in Jilin Province, NE China and its geological significance. *Resour. Geol.* **2014**, *64*, 247–261. [CrossRef]
9. Deng, J.; Yuan, W.; Carranza, E.J.M.; Yang, L.; Wang, C.; Yang, L.; Hao, N. Geochronology and thermochronometry of the Jiapigou gold belt, northeastern China: New evidence for multiple episodes of mineralization. *J. Asian Earth Sci.* **2014**, *89*, 10–27. [CrossRef]
10. Zhang, Y.; Xing, S.W.; Song, Q.H.; Wang, Y.; Yu, Z.T.; Du, X.H.; Ma, Y.B.; Zhang, Z.J. Re–Os and U–Pb geochronology of porphyry and skarn types copper deposits in Jilin Province, NE China. *Resour. Geol.* **2015**, *65*, 394–404. [CrossRef]
11. Zhou, L.L.; Zeng, Q.D.; Liu, J.M.; Friis, H.; Zhang, Z.L.; Duan, X.X. Ore genesis and fluid evolution of the Daheishan giant porphyry molybdenum deposit, NE China. *J. Asian Earth Sci.* **2015**, *97*, 486–505. [CrossRef]
12. Wang, Z.G.; Wang, K.Y.; Wan, D.; Yassa, K.; Yang, T.N.; Liang, Y.H. Metallogenic age and hydrothermal evolution of the Jidetun Mo deposit in central Jilin Province, northeast China: Evidence from fluid inclusions, isotope systematics, and geochronology. *Ore Geol. Rev.* **2017**, *89*, 731–751. [CrossRef]
13. Yang, Q. Late Paleozoic to Early Mesozoic Copper-Gold Polymetallic Metallogeny and Metallogenic Regularity in Central Jilin Province, Northeast China. Ph.D. Thesis, Jilin University, Changchun, China, 2020. (In Chinese with English Abstract)
14. Ren, Y.S.; Ju, N.; Chen, C.; Yang, Q.; Shang, Q.Q.; Lai, K. Late Paleozoic VMS-type deposit and its tectonic significance in eastern Jilin Province, NE China. *Acta Mineral. Sin.* **2015**, *35*, 493. (In Chinese)
15. Lu, S.Y.; Ren, Y.S.; Yang, Q.; Sun, Z.M.; Hao, Y.J.; Sun, X.H. Ore genesis for stratiform ore bodies of the Dongfengnanshan copper polymetallic deposit in the Yanbian Area, NE China: Constraints from LA-ICP-MS in situ trace elements and sulfide S–Pb isotopes. *Acta Geol. Sin. (Engl. Ed.)* **2019**, *93*, 1591–1606. [CrossRef]
16. Hou, H.N. Tectonic Setting and Metallogenic Significance of Late Paleozoic Volcanic Rock Series in the Yanbian Area, NE China. Ph.D. Thesis, Jilin University, Changchun, China, 2020. (In Chinese with English Abstract)
17. Wang, Z.G.; Wan, D.; Wang, K.Y.; Konare, Y.; Liang, Y.H. Isotope systematics and fluid inclusion studies of the Hongtaiping Cu–Pb–Zn deposit in Yanbian, NE China: Implications for ore genesis. *Geol. J.* **2020**, *55*, 6912–6935. [CrossRef]
18. Chang, J.J. Study on Geological Characteristics and Genesis of Xiaohongshilazi Lead–Znic Deposit, Panshi, Jilin Province. M.S. Thesis, Jilin University, Changchun, China, 2016. (In Chinese with English Abstract)
19. Li, Y. Ore Genesis and Tectonic Setting of Xiaohongshilazi Lead-Zinc Deposit in Panshi Area, Jilin Province. M.S. Thesis, Jilin University, Changchun, China, 2017. (In Chinese with English Abstract)
20. Yang, Q.; Ren, Y.S.; Li, Y.; Hao, Y.J.; Li, J.M.; Shang, Q.Q.; Sun, X.H. Age and tectonic setting of mesothermal magmatic hydrothermal vein-type Pb–Zn–(Ag) mineralization in the Xiaohongshilazi deposit, central Jilin Province, NE China. *Res. Geol.* **2020**, *70*, 70–88. [CrossRef]
21. Zhu, Y.Y.; Zhang, J.Q.; Cao, J.F. Geological features and prospecting criteria of the Xiaohongshilazi silver lead-zinc deposit. *Jilin Geol.* **2012**, *31*, 55–59, (In Chinese with English Abstract)
22. Cao, J.F.; Sun, Z.Y.; Xue, X.G. The characteristics and significance of the Pb and Zn massive sulfide deposits in Xiaohongshilazi, Panshi City, Jilin Province. *J. Changchun Inst. Tech. (Nat. Sci. Ed.)* **2012**, *13*, 90–94. (In Chinese with English Abstract)
23. Zhang, X.Z.; Zhou, J.B.; Chi, X.G.; Wang, C.W.; Hu, D.Q. Late Paleozoic tectonic-sedimentation and petroleum resources in Northeast China. *J. Jilin Univ. (Earth Sci. Ed.)* **2008**, *38*, 719–725. (In Chinese with English Abstract)
24. Peng, X.D.; Zhang, M.S.; Li, X.M. The evolution of Paleozoic tectonic paleogeography in Jilin and Heilongjiang orogenic belt. *World Geol.* **1999**, *18*, 24–28. (In Chinese with English Abstract)
25. Peng, Y.J.; Zhao, C.B. The evolution of the Paleo Jihei orogenic belt and accretion of the continental crust. *Jilin Geol.* **2001**, *20*, 1–9. (In Chinese with English Abstract)
26. Zhang, X.Z.; Ma, Y.X.; Chi, X.G.; Zhang, F.X.; Sun, Y.W.; Guo, Y.; Zeng, Z. Discussion on Phanerozoic tectonic evolution in Northeast China and eastern Inner Mongolia. *J. Jilin Univ. (Earth Sci. Ed.)* **2012**, *42*, 1269–1285. (In Chinese with English Abstract)
27. Jia, D.C.; Hu, R.Z.; Lu, Y.; Qiu, X.L. Collision belt between the Khanka block and the North China block in the Yanbian Region, Northeast China. *J. Asian Earth Sci.* **2004**, *23*, 211–219.
28. Li, J.Y. Permian geodynamic setting of Northeast China and adjacent regions: Closure of the Pale-Asian Ocean and subduction of the Paleo-Pacific Plate. *J. Asian Earth Sci.* **2006**, *26*, 207–224. [CrossRef]
29. Lin, W.; Faure, M.; Nomade, S.; Shang, Q.H.; Renne, P.R. Permian-Triassic amalgamation of Asia: Insights from Northeast China sutures and their place in the final collision of North China and Siberia. *Comptes Rendus Geosci.* **2008**, *340*, 190–201. [CrossRef]

30. Cao, H.H.; Xu, W.L.; Pei, F.P.; Wang, Z.W.; Wang, F.; Wang, Z.J. Zircon U–Pb geochronology and petrogenesis of the Late Paleozoic–Early Mesozoic intrusive rocks in the eastern segment of the northern margin of the North China Block. *Lithos* **2013**, *170–171*, 191–207. [CrossRef]
31. Chen, B.; Jahn, B.M.; Tian, W. Evolution of the Solonker suture zone: Constraints from zircon U–Pb ages, Hf isotopic ratios and whole-rock Nd-Sr isotope compositions of subduction and collision-related magmas and forearc sediments. *J. Asian Earth Sci.* **2009**, *34*, 245–257. [CrossRef]
32. Zhou, J.B.; Wilde, S.A. The crustal accretion history and tectonic evolution of the NE China segment of the Central Asian Orogenic Belt. *Gondwana Res.* **2013**, *23*, 1365–1377. [CrossRef]
33. Sengör, A.M.C.; Natal'in, B.A. Paleotectonics of Asia: Fragments of a synthesis. In *The Tectonic Evolution of Asia*; Yin, A., Harrison, M., Eds.; Cambridge University Press: London, UK, 1996; pp. 486–640.
34. Zhang, Y.B.; Wu, F.Y.; Wilde, S.A.; Zhai, M.G.; Lu, X.P.; Zhang, X.F. Geochronology and tectonic implications of the "Proterozoic" Seluohe Group at the Northern margin of the North China Craton. *Int. Geol. Rev.* **2008**, *50*, 135–153. [CrossRef]
35. Wang, Z.J. Late Paleozoic−Triassic Tectonic Evolution of Eastern Segment of the Southern Margin of the Xing'an–Mongolia Orogenic Belt: Evidence from Detrital Zircon U-Pb Geochronology and Igneous Rock Associations. Ph.D. Thesis, Jilin University, Changchun, China, 2016. (In Chinese with English Abstract)
36. Hou, K.J.; Li, Y.H.; Tian, Y.R. In situ U−Pb zircon dating using, laser ablation–multiion counting-ICP–MS. *Miner. Deposits* **2009**, *28*, 481–492. (In Chinese with English Abstract)
37. Griffin, W.L.; Powell, W.J.; Pearson, N.J.; O'Reilly, S.Y. GLITTER: Data reduction software for laser ablation ICP–MS. In *Laser Ablation–ICP–MS in the Earth Sciences: Current Practices and Outstanding Issues*; Mineralogical Association Canada Short Course; Sylvester, P., Ed.; Mineralogical Association Canada: Quebec City, QC, Canada, 2008; Volume 40, pp. 308–311.
38. Ludwig, K.R. User's manual for Isoplot 3.0: A geochronological toolkit for Microsoft Excel. *Berkeley Geochrono. Cent. Spec. Publ.* **2003**, *4*, 1–70.
39. Anderson, T. Correction of common lead in U–Pb analyses that do not report ^{204}Pb. *Chem. Geol.* **2002**, *192*, 59–79. [CrossRef]
40. Qi, L.; Zhou, M.F. Platinum-group elemental and Sr-Nd-Os isotopic geochemistry of Permian Emeishan flood basalts in Guizhou Province, SW China. *Chem. Geol.* **2008**, *248*, 83–103. [CrossRef]
41. Belousova, E.A.; Griffin, W.L.; O'Reilly, S.Y. Igneous zircon: Trace element composition as an indicator of source rock type. *Contrib. Mineral. Petrol.* **2002**, *143*, 602–622. [CrossRef]
42. Hoskin, P.W.O.; Schaltegger, U. The composition of zircon and igneous and metamorphic petrogenesis. *Rev. Mineral. Geochem.* **2003**, *53*, 27–62. [CrossRef]
43. Qiu, K.F.; Marsh, E.; Yu, H.C.; Pfaff, K.; Gulbransen, C.; Gou, Z.Y.; Li, N. Fluid and metal sources of the Wenquan porphyry molybdenum deposit, Western Qinling, NW China. *Ore Geol. Rev.* **2017**, *86*, 459–473.
44. Boynton, W.V. Geochemistry of the rare earth elements: Meteorite studies. In *Rare Earth Element Geochemistry*; Henderson, P., Ed.; Elsevier: Amsterdam, The Netherlands, 1984; pp. 63–114.
45. Sun, S.S.; McDonough, W.F. Chemical and isotopic systematics of oceanic basalts: Implications for mantle composition and processes. *Geol. Soc.* **1989**, *42*, 313–345.
46. Winchester, J.A.; Floyd, P.A. Geochemical discrimination of different magma series and their differentiation products using immobile elements. *Chem. Geol.* **1977**, *20*, 325–343. [CrossRef]
47. Hastie, A.R.; Kerr, A.C.; Pearce, J.A.; Mitchell, S.F. Classification of altered volcanic island arc rocks using immobile trace elements: Development of the Th–Co discrimination diagram. *J. Petrol.* **2007**, *48*, 2341–2357. [CrossRef]
48. Peccerillo, A.; Taylor, A.R. Geochemistry of Eocene calc-alkaline volcanic rocks from the Kastamonu area, Northern Turkey. *Contrib. Miner. Petrol.* **1976**, *58*, 63–81.
49. Cao, H.H. Geochronology and Geochemistry of the Late Paleozoic-Early Mesozoic Igneous Rocks in the Eastern Segment of the Northern Margin of the North China Block. Ph.D. Thesis, Jilin University, Changchun, China, 2013. (In Chinese with English Abstract)
50. Yu, Q.; Ge, W.C.; Yang, H.; Zhao, G.C.; Zhang, Y.L.; Su, L. Petrogenesis of late Paleozoic volcanic rocks from the Daheshen Formation in central Jilin Province, NE China, and its tectonic implications: Constraints from geochronology, geochemistry and Sr-Nd-Hf isotopes. *Lithos* **2014**, *192/195*, 116–131.
51. Li, D.J. *Stratigraphy (Lithostratic) of Jilin Province*; China University of Geosciences Press: Wuhan, China, 1997; pp. 1–324. (In Chinese)
52. Lu, S.Y.; Ren, Y.S.; Hao, Y.J.; Hou, H.H.; Yang, Q. Two-phase mineralization of Hongtaiping Cu polymetallic deposit in Yanbian area (NE China): Evidence from sulfde Rb–Sr dating and in-situ trace element analysis. *Ore Geol. Rev.* **2021**, *137*, 104295.
53. Gill, J.B. Early geochemical evolution of an oceanic island arc and backarc: Fiji and the South Fiji Basin. *J. Geol.* **1987**, *95*, 589–615. [CrossRef]
54. Nurlu, N.; Akinci, A.C.; Kohút, M. Geochemistry and geochronology of Middle Eocene subduction-related felsic volcanics in the Misis-Andirin Complex of the Southeast Anatolian Orogenic Belt. *Geosci. J.* **2023**. [CrossRef]
55. Sünger, A.; Akyıldız, M.; Nurlu, N. Significance of the Felsic Sub–Volcanics in Development of Related Au–Ag Deposits at Maden Village (Bolkar Mountain Region), South Turkey: Constraints from Whole–Rock Geochemistry, Geochronology and Pb-S Isotopes. *Geotectonics* **2022**, *56*, 361–381.

56. Baker, M.B.; Hirschmann, M.M.; Ghiorso, M.S.; Stolper, E.M. Compositions of near-solidus peridotite melts from experiments and thermodynamic calculations. *Nature* **1995**, *375*, 308–311. [CrossRef]
57. Kelemen, P.B.; Hanghj, K.; Greene, A.R. One view of the geochemistry of subduction-related magmatic arcs, with an emphasis on primitive andesite and lower crust. *Trea. Geochem.* **2007**, *3*, 1–70.
58. Rollinson, H.R. *Using Geochemical Data: Evaluation, Presentation, Interpretation*; Longman Publishing Group: London, UK, 1993; pp. 1–384.
59. Rapp, R.P.; Watson, E.B. Dehydration melting of metabasalt at 8 ~ 32 kbar: Implications for continental growth and crust-mantle recycling. *J. Petrol.* **1995**, *36*, 891–931. [CrossRef]
60. Yang, Q.; Ren, Y.S.; Huizenga, J.M.; Li, J.M.; Wang, E.D.; Wang, X.; Wang, B. Geological signifcance of Early Triassic porphyry Cu mineralization in the eastern Xar Moron–Changchun Metallogenic Belt, northeast China: A case study of the newly-discovered Guokuidingzi Cu deposit. *Ore Geol. Rev.* **2021**, *133*, 104092.
61. Collins, W.J.; Beams, S.D.; White, A.J.R.; Chappell, B.W. Nature and origin of A-type granites with particular reference to southeastern Australia. *Contrib. Mineral. Petrol.* **1982**, *80*, 189–200.
62. Whalen, J.B.; Currie, K.L.; Chappell, B.W. A-type granites: Geochemical characteristics, discrimination and petrogenesis. *Contrib. Mineral. Petrol.* **1987**, *95*, 407–419. [CrossRef]
63. Bonin, B. A-type granites and related rocks: Evolution of a concept, problems and prospects. *Lithos* **2007**, *97*, 1–29. [CrossRef]
64. Lu, S.Y.; Ren, Y.S.; Yang, Q.; Hao, Y.J.; Zhao, X. Petrogenesis and tectonic implication of the Hongtaiping high-mg diorite in the Wangqing area, NE China: Constraints from geochronology, geochemistry and Hf isotopes. *Minerals* **2022**, *12*, 1002. [CrossRef]
65. Lü, L.S.; Mao, J.W.; Li, H.B.; Pirajno, F.; Zhang, Z.H.; Zhou, Z.H. Pyrrhotite Re-Os and SHRIMP zircon U–Pb dating of the Hongqiling Ni-Cu sulfide deposits in Northeast China. *Ore Geol. Rev.* **2011**, *43*, 106–119.
66. Pearce, J.A.; Harris, N.B.W.; Tindle, A.G. Trace element discrimination diagrams for the tectonic interpretation of granitic rocks. *Petrol.* **1984**, *25*, 956–983. [CrossRef]